*Journal of Science and Technology* ***55*** *(1B) (2017) 266–275*

# SYNTHESIS OF ZINC OXIDE/GRAPHENE OXIDE NANOCOMPOSITES AS ANTIBACTERIAL MATERIALS AGAINST *STAPHYLOCOCCUS AUREUS* AND *ESCHERICHIA COLI*

**Nguyen Huu Hieu[1, 2, *], Dang Thi Tuong Vi[2]**

[1] *Faculty of Chemical Engineering, HCMUT–VNUHCM*
*268 Ly Thuong Kiet Street, Ward 14, District 10, Ho Chi Minh City, Vietnam*

[2] *Key Laboratory of Chemical Engineering and Petroleum Processing, HCMUT–VNUHCM*
*268 Ly Thuong Kiet Street, Ward 14, District 10, Ho Chi Minh City, Vietnam*

[*]Email: *nhhieubk@hcmut.edu.vn*

Received: 30 December 2016; Accepted for Publication: 9 March 2017

## ABSTRACT

New materials with good antibacterial activity and less toxicity to other species have attracted numerous research interests. Modified Hummers method was used for preparing graphene oxide (GO). Zinc oxide/graphene oxide (ZnO/GO) nanocomposites were synthesized with three different ratios (0.5:1, 1:1, and 2:1) by solution precipitation method. The ZnO/GO nanocomposites were characterized by Fourier transform infrared spectroscopy, X–ray diffraction, Raman spectroscopy, Brunauer–Emmett–Tellerspecific surface area, and transmission electron microscopy image. The characterization results showed that ZnO nanoparticles with a mean size of 12–18 nm were randomly decorated on the surfaces and edges of GO sheets. ZnO/GO 1:1 with a high specific surface area of 65 $m^2/g$ was obtained. The antibacterial activity of ZnO, GO, and ZnO/GO was tested against Gram negative bacteria *escherichia coli (E. coli)* and Gram positive bacteria *staphylococcus aureus (S. aureus)* using well diffusion method. The test results confirmed that antibacterial activity of ZnO/GO was higher than that of GO and ZnO. Additionally, the ZnO/GO with the ratio of 1:1 is the strongest activity and more active against *S. aureus* than against *E. coli* and minimal inhibitory concentration (MIC) value of ZnO/GO 1:1 is 80 µg/mL for *S. aureus* and 160 µg/mL for *E. coli.* This novel nanocomposite could be used as a potential material for antimicrobial application.

*Keywords:* graphene oxide, ZnO, antibacterial activity, *E. coli*, *S. aureus*.

## 1. INTRODUCTION

Bacterial infectious diseases are a serious health problem that has drawn the public attention in worldwide as a human health threat, which extends to economic and social complications. Biocidal nanomaterials are an attractive field of science that has the capability to other things such as enhance medical devices [1], wastewater treatment [2], food packaging [3],

synthetic textiles [4], and dentistry [5]. Development of novel and efficient antibacterial agents is urgently required due to the growing antibacterial resistance spectrum of bacterial infections. The control of bacterial growth is one of the most challenging environmental issues since surfaces exposed to media rich in microorganisms can be damaged or lose their functionality. The effects of microorganisms on their environment can be beneficial or harmful or in apparent with regard to human measure or observation.

Zinc oxide (ZnO) has the inherent advantage of broad antibacterial activities [6, 7], antifungal [8]. Nano sized ZnO can interact with the bacterial surface or with the bacterial core where it inside the cell, and subsequently exhibits distinct bactericidal mechanisms [9]. Interestingly, this aspect necessitated their usage as antibacterial agents, noxious to microorganisms, and hold good biocompatibility to human cells [10]. Synthesis of ZnO particles with a precipitation method in alcohol solution is the most commonly used and promising low–cost route [11–13]. However, ZnO particles aggregate easily in solution due to van der Waals forces and surface effects [14]. Therefore, the surface of ZnO particles must be modified with an organic reagent or stable polymers to decrease aggregation [15].

Graphene oxide (GO) is a two–dimensional material with intriguing properties such as large surface–to–volume ratio, robust optical transparency, and electronic transport capabilities [16–18]. Microscopic characterization has revealed that graphene oxide has a layered structure in which carbon atoms twist to form tetrahedrons, which creates wrinkles and grooves on the surface [19]. Chemically functionalized groups on the π–conjugated planes of graphene oxide allow easy anchoring of covalently bonded micrometer and nanometer particles onto graphene oxide [20].

Several studies have demonstrated the strong antimicrobial activity of GO against a wide variety of microorganisms, including Gram–positive and negative bacterial pathogens, phytopathogens, and biofilm forming microorganisms. The antimicrobial activity of GO is thought to be mediated by physical and chemical interactions when sheets come in direct contact with bacterial cells [21]. In this study, ZnO/GO nanocomposites were examined with the antibacterial activity and MIC with *S. aureus* and *E. coli*.

## 2. MATERIALS AND METHODS

### 2.1. Materials

Graphite powder (particle size < 50 μm, density: 20–30 g/100 mL) was purchased from Sigma–Aldrich (Germany); potassium permanganate (> 99.5 wt%) was purchased from Duc Giang Detergent Chemical JSC (Vietnam); ammonia sulfuric acid (98 wt%), sodium nitrate (99 wt%), zinc acetate (99 wt%), and ethylene glycol were purchased from Xilong Chemical (China).-Mueller–Hinton Agar (MHA) was purchased from Vietnam. All chemicals were used without further purification. *E. coli* and *S. aureus* were purchased from Pasteur Institute in Ho Chi Minh City.

### 2.2. Methods

#### *2.2.1. Preparation of GO*

Graphite oxide (GiO) was prepared from graphite by modified Hummers' method [22]. According to this method, 1 g of graphite and 0.5 g of sodium nitrate were mixed together and added in 60 mL concentrated sulfuric acid under constant stirring at a temperature of less than 5

°C. For the first oxidation, 3 g of $KMnO_4$ was added gradually to the above solution while maintaining the temperature at less than 20 °C. Then, the mixture was heated to 35 °C and sonicated in an ultrasound bath (500 W) for 2 h. For the second oxidation, 3 g of $KMnO_4$ were added to the mixture followed by a sonication at 35 °C for 4 h. Then, 400 mL of distilled water were added and the solution placed at room temperature. In order to ensure the completion of the reaction with $KMnO_4$, the suspension was further treated with 30% hydrogen peroxide solution until light yellow color appeared. After that, the mixture was centrifuged, washed with distilled water until pH 6, and dried at 80 °C to obtain GiO. The obtained GiO was dispersed in distilled water to achieve a concentration of 0.5 mg/mL $H_2O$. Subsequently, the GiO suspension was exfoliated by sonicating for 12 h to obtain GO. Finally, GO was centrifuged and dried at room temperature.

*2.2.2. Preparation of ZnO*

Zinc acetate (3.36 g) and sodium hydroxide (4 g) were dissolved in succession into 160 mL distilled water heated to 120 °C under continuous stirring. The solution was stirred at 800 rpm and maintained at a temperature of 120 °C for 45 min. After that, the mixture was centrifuged, washed with distilled water until pH 6, and dried at 80 °C. Then the samples were annealed in air at 500 °C for 10 min.

*2.2.3. Preparation of ZnO/GO*

ZnO/GO nanocomposite was prepared with three different ZnO to GO ratios (0.5:1, 1:1, and 2:1). The samples were denoted as follows: ZnO/GO 0.5:1, ZnO/GO 1:1, and ZnO/GO 2:1 by solution precipitation method. Accordingly, 0.05 g of GO and 0.287 g of $ZnC_4H_6O_4.2H_2O$ were dissolved in 40 mL of ethylene glycol under ultrasonication for 1 h. Subsequently, the mixture was heated to 120 °C under vigorous stirring. Then, 0.102 g of NaOH dissolved in 5 mL of distilled water was added to the mixture. After stirring for 2 h, the mixture was allowed to cool to room temperature and was then centrifuged and washed with absolute ethanol and deionized water several times. Finally, the obtained ZnO/GO was dried at room temperature.

*2.2.4. Antibacterial test*

Antibacterial activity of materials was tested by the well diffusion method. The sterilized nutrient agar was poured (20 mL/plate) onto the Petri plates and left for a while till the agar got solidified. Two pathogenic strains of *E. coli* (gram negative) and *S. aureus* (gram positive) were taken and made into cultures. Fresh overnight cultures of inoculum (100 µL) of each culture were spread onto nutrient agar plate's surface evenly in four different petri plates respectively, the wells were cast by pore (3 mm diameter). The samples along with standard antibiotic (ampicillin) were loaded with equal volume (10 µL) on the plates. Control plate consists of distilled water and antibiotic drugs. The square plates were incubated at room temperature for 19–24 h. Activity was clearly visible from 19 h to 24 h on the plates. A zone of inhibition was measured and the sample of the ZnO/GO showing maximum antimicrobial activity was noted.

The lowest concentration of material that inhibits the growth of an organism was defined as the minimum inhibitory concentration (MIC). The well diffusion method was employed to determine the MIC of the ZnO/GO nanocomposite. Each of the 36 wells was filled with 100 µL of the liquid Muller Hinton broth medium. Into the test well number 1, 100 µL solution containing 640 µg/mL of ZnO/GO that had been sonicated at room temperature and at 10 min, was already added and mixed thoroughly with the culture medium. Then, 1 mL of the content of the test well number 1 was added to test well number 2 and mixed completely. This process was

performed serially to test tube number 12. After that, 25 µL standard microbial suspensions was added into the wells number 13 to 24.

### 2.3. Analytical methods

Fourier transform infrared (FTIR) spectra were recorded in the 4000–400 $cm^{-1}$ range with a Bruker FTIR Alpha–E spectrometer (The Key Laboratory of Chemical Engineering–Petroleum Processing, HCMUT–VNUHCM). X–ray diffraction (XRD) patterns were observed on a Bruker D8 Advanced powder diffractometer system using Cu–Kα radiation (National Key Lab for Polymer & Composite Materials–VNUHCM). Raman spectra were recorded using LabRam micro–Raman spectrometer with an excitation wavelength of 632 nm (He–Ne laser) (Institute of Nanotechnology – VNUHCM). Brunauer–Emmett–Teller (BET) specific surface area and pore size distribution were measured by Quantachrome's NOVA 1200e (MANAR Center–VNUHCM). Before measurement, each sample was outgassed under vacuum at 150 °C for 1 h. Transmission electron microscopy (TEM) image was obtained using a JEOL JEM 1010 microscope at an acceleration voltage of 100 kV (National Key Lab for Polymer & Composite Materials–VNUHCM)

## 3. RESULTS AND DISCUSSION

### 3.1. FTIR analysis

The functional groups of GO, ZnO, ZnO/GO 0.5:1, ZnO/GO 1:1, and ZnO/GO 2:1 were analyzed through FTIR spectra as shown in Figure 1. In the FTIR spectrum of GO the representative peaks of the oxygen–containing functional groups appear at 1735 $cm^{-1}$ (C=O), 1388 $cm^{-1}$ (C–OH), and 1060 $cm^{-1}$ (C–O–C), respectively. The peak at 1622 $cm^{-1}$ is assigned to the skeletal vibration of the GO sheets [23]. In the spectra of ZnO/GO 0.5:1, ZnO/GO 1:1, and ZnO/GO 2:1, those peaks of oxygen–containing groups red–shift and their intensity also changes. The appearance of the characteristic peak at 1627 $cm^{-1}$ attributed to aromatic C=C vibrations, reveal some structural change of GO, the unfolding of wrinkled GO sheets, in the second step of preparing ZnO/GO composite material. These changes may be related to some chemical interaction between GO and ZnO. In addition, the strong band at about 441 $cm^{-1}$ is attributed to Zn–O.

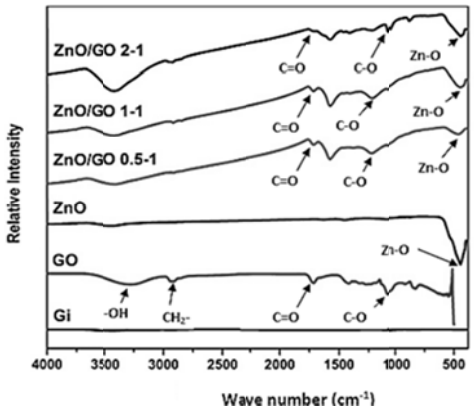


*Figure 1*. FTIR spectra of ZnO, GO, ZnO/GO 0.5:1, ZnO/GO 1:1, and ZnO/GO 2:1.

### 3.2. XRD analysis

The phase and structure of GO, ZnO (JCPDS card No. 36–1451), ZnO/GO 0.5:1, ZnO/GO 1:1, and ZnO/GO 2:1 nanocomposite were investigated by XRD, as shown in Figure 2. As can be observed the XRD pattern of GO shows a sharp peak at 2θ = 10.8°, corresponding to the (001) reflection of GO [24]. Moreover, the diffraction peaks at 31.7°, 34.4°, 36.3°, 47.5°, 56.5°, 62.8°, and 68.0° can be assigned to the (100), (002), (101), (102), (110), (103), and (112) planes of the crystalline ZnO, respectively [7]. However, there is no characteristic peak of the (001) reflection of GO, ZnO/GO 0.5:1, the ZnO/GO 0.5:1, ZnO/GO 1:1 and ZnO/GO 2:1 in the nanocomposite. This indicates that GO was reduced by the ethylene glycol at high temperature during the formation of ZnO nanoparticles [25].

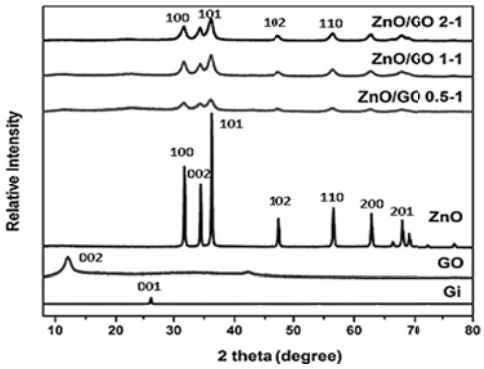


*Figure 2*. XRD patterns of ZnO, GO, ZnO/GO 0.5:1, ZnO/GO 0.5:1, ZnO/GO 1:1, and ZnO/GO 2:1.

### 3.3. Raman spectra

In this study, we describe characteristic properties of the material by Raman spectroscopy. In Figure 3, Gi spectrum has two peaks at D–band (1332 $cm^{-1}$) and G–band (1584 $cm^{-1}$) and the 2D (2650–2700 $cm^{-1}$) peaks due to optical vibration of carbon graphite electrode. Raman spectra of ZnO/GO 0.5:1, ZnO/GO 1:1, and ZnO/GO 2:1 showed two bands at 1345 $cm^{-1}$ and 1582 $cm^{-1}$ corresponding to the disordered (D) band and graphite (G) band of carbon materials. The structural changes from GO to ZnO/GO could be observed by comparing the intensity ratio of the D and G bands ($I_D/I_G$). Table 1 shows that $I_D/I_G$ ratios for GO and ZnO/GO (2:1) were 1.04 and 1.14, respectively. This result indicates that the ratio $I_D/I_G$, for GO is lower than for ZnO/GO (2:1), implying, perhaps, that GO has fewer defects than ZnO/GO (1:1) [26, 27].

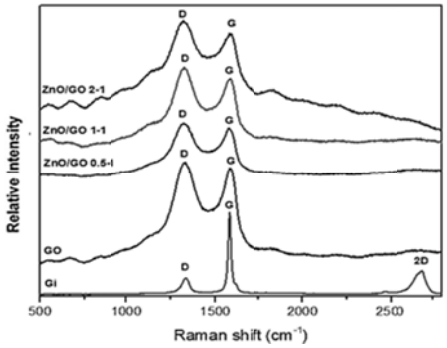


*Figure 3.* Raman spectra of Gi, GO, ZnO/GO 0.5:1, ZnO/GO 1:1, and ZnO/GO 2:1.

*Table 1.* Ratio of peak intensities ($I_D/I_G$) of various materials.

| | GO | ZnO/GO | | |
|---|---|---|---|---|
| | | 0.5:1 | 1:1 | 2:1 |
| $I_D/I_G$ | 1.04 | 1.06 | 1.09 | 1.14 |

### 3.4. BET specific surface areas

From the adsorption branch of the isotherms, the specific surface areas of ZnO/GO 0.5:1, ZnO/GO 1:1, and ZnO/GO 2:1 are calculated through a BET method [28], which was higher compared to other materials, as shown in Table 2. A higher surface area of ZnO/GO nanocomposite than ZnO and GO is expected. The surface area of ZnO/GO (1:1) is the highest at 65.158 $m^2/g^{-1}$. These results suggest that the ZnO/GO 1:1 nanocomposites are characterized by mesoporous structures. The pore size distribution curves calculated pore sizes in the range from 1 to 10 nm. In contrast to the ZnO/GO nanocomposites, ZnO/GO 0.5:1, ZnO/GO 2:1 show a much broader pore size distribution.

*Table 2*. The BET surface area of various materials.

| No. | Materials | BET surface area ($m^2/g$) |
|---|---|---|
| 1 | ZnO/GO 0.5:1 | 8.438 |
| 2 | ZnO/GO 1:1 | 65.158 |
| 3 | ZnO/GO 2:1 | 31.441 |

### 3.5. TEM images

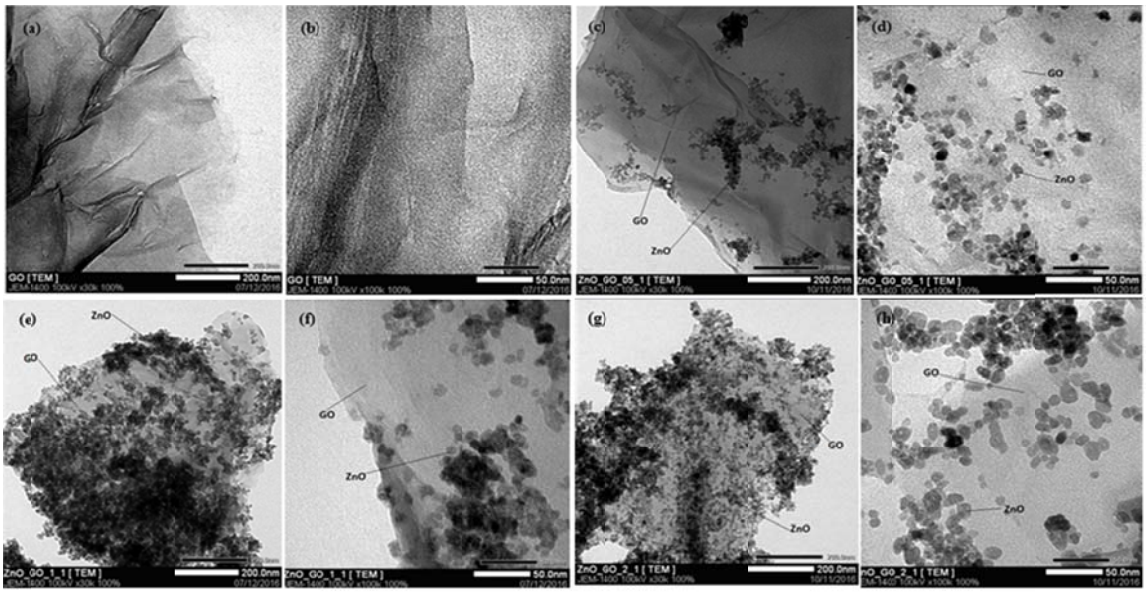


*Figure 4.* TEM images of GO (a, b), ZnO/GO 0.5:1 (c, d), ZnO/GO 1:1 (e, f), and ZnO/GO 2:1 (g, h).

Figure 4 shows TEM images with different sizes of ZnO/GO 0.5:1, ZnO/GO 1:1, and ZnO/GO 2:1 nanocomposite, which are the light–gray thin films are the GO sheets, and the dark regions on the GO background are due to the presence of ZnO particles. It can be clearly seen in

Figure 4 that the exfoliated GO sheet was decorated with ZnO aggregates with sizes of 12–18 nm, whereas some of the flower–like ZnO microstructures on GO sheets were crushed into fragments because of the ultrasonic treatment before TEM observation. Moreover, the loaded flower–like ZnO particles were mainly located at the edge of the GO sheets, which might result from the aggregation of ZnO particles that confined their efficient dispersion on GO sheets. The result is consistent with those of previous studies [29].

### 3.6. Antibacterial activity

The antibacterial activities of ZnO, GO, ZnO/GO (0.5:1), ZnO/GO (1:1), and ZnO/GO (2:1) were determined by the formation of a zone. A zone of inhibition is the area on an agar plate where the growth of a control organism is prevented by an antibiotic usually placed on the agar surface. If the test organism is susceptible to the antibiotic, it will not grow where the antibiotic is present. The size of the zone of inhibition is a measure of the compound's effectiveness, the larger the clear area around the antibiotic, the more effective the compound.

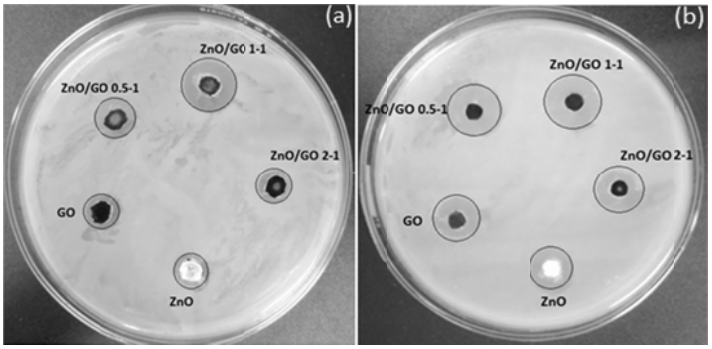


*Figure 5.* A zone of inhibition formation against *S. aureus* (a) and *E. coli* (b).

The activity of ZnO, GO, ZnO/GO 0.5:1, ZnO/GO 1:1, and ZnO/GO 2:1 was observed by the formation of a zone of inhibition after 24 h at concentration of 500 µg/mL. The presence of a zone of inhibition confirmed inhibitory activity of ZnO, GO, ZnO/GO 0.5:1, ZnO/GO 1:1, and ZnO/GO 2:1. The zone of inhibitions of *S. aureus* and *E. coli* bacteria is given in Figure 5. The clear a zone surrounding the sample in the remaining plates shows the activity of the sample. Figure 5 shows the petri dishes with samples of ZnO, GO, ZnO/GO 0.5:1, ZnO/GO 1:1, and ZnO/GO 2:1 with *S. aureus* and *E. coli.* The size of this zone depends on how effective the antibiotic is at stopping the growth of the bacterium. The result showed the antibacterial activity of ZnO/GO 1:1 is strongest. In addition, Table 3 showed the antibacterial activity of ZnO/GO 1:1 nanocomposite for *S. aureus* was higher than *E. coli*.

The MIC values of ZnO/GO 1:1 is 80 µg/mL for *S. aureus* (Figure 6) and 160 µg/mL for *E. coli* (Figure 7) are presented in Table 4. There are two explanations as to why gram–positive bacteria are less susceptible than gram–negative bacteria. The first involves the charge of peptidoglycan molecules in the bacterial cell wall. Gram–positive bacteria have more peptidoglycan than gram–negative bacteria because of their thicker cell walls, and because peptidoglycan is negatively, more ZnO/GO may get trapped by peptidoglycan in gram–positive bacteria than in gram–negative bacteria. The decreased susceptibility of gram–positive bacteria can also simply be explained by the fact that the cell wall of gram–positive bacteria is thicker than that of gram–negative bacteria. It would allow the penetration of a greater number of

negatively charged free radicals such as superoxide anions and hydroxyl radicals, into the cell, and death of the cell.

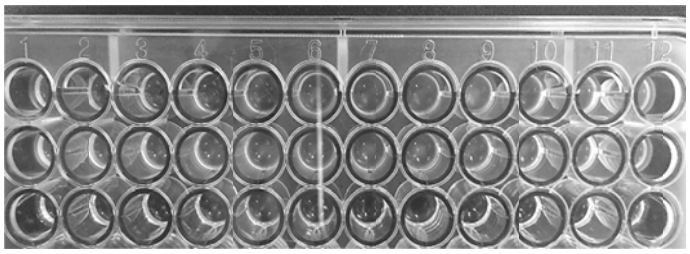

*Figure 6.* MIC test of ZnO/GO for against *S. aureus.*

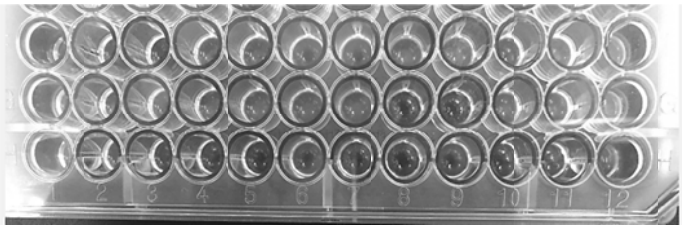

*Figure 7.* MIC test of ZnO/GO for *E. coli.*

*Table 3.* A zone of inhibition of ZnO, GO, ZnO/GO 0.5:1, ZnO/GO 1:1, and ZnO/GO 2:1 with *S. aureus* and *E. coli.*

| No. | Sample | A zone of Inhibition (mm) | |
|---|---|---|---|
| | | ***S. aureus*** | ***E. coli*** |
| 1 | Zn | 10 | 8 |
| 2 | GO | 11 | 9 |
| 3 | ZnO/GO 0.5:1 | 15 | 11 |
| 4 | ZnO/GO 1:1 | 20 | 17 |
| 5 | ZnO/GO 2:1 | 13 | 9 |

*Table 4.* MIC of ZnO/GO 1:1 with *S. aureus* and *E. Coli.*

| No. | Bacterial strain | MIC |
|---|---|---|
| 1 | *S. aureus* | 80 µg/ml |
| 2 | *E. coli* | 160 µg/ml |

## 4. CONCLUSIONS

ZnO/GO nanocomposites were prepared with three different ratios (0.5:1, 1:1, and 2:1) by solution precipitation method. The FTIR and XRD results showed the characteristic diffraction peaks and the functional groups of GO and ZnO/GO. The Raman spectra confirmed that GO has the two main characteristic peaks (D–band and G–band). The BET specific area of ZnO/GO 1:1 was 65.158 $m^2/g$. The TEM images revealed the ZnO nanoparticles with a size distribution of 12–18 nm decorated onto surfaces of GO sheets. The antibacterial properties of ZnO, GO, ZnO/GO 0.5:1, ZnO/GO 1:1, and ZnO/GO 2:1 were tested against *E. coli* and *S. aureus* using

well diffusion method. The test results confirmed that antibacterial activity of ZnO/GO was higher than that of GO and ZnO. In addition, ZnO/GO with the ratio of 1:1 was the strongest activity and more active against *S. aureus* than against *E. coli.* Additionally, MIC value of ZnO/GO 1:1 is 80 μg/mL for *S. aureus* and 160 μg/mL for *E. coli.* This novel nanocomposite could be used as a potential material for the antimicrobial application.

## REFERENCES


1. Zhao L., Wang H., Huo K., Cui L., Zhang W. – Antibacterial nanostructured titania coating incorporated with silver nanoparticles, Biomaterials **32** (2011) 5706–5716
2. Zhang M., Zhang K., Gusseme B. D., Verstraete W. – Biogenic silver nanoparticles (bio–Ag 0) decrease biofouling of bio–Ag/PES nanocomposite membranes, Water Research **46** (2012) 2077–2087.
3. Prombutara P., Kulwatthanasal Y., Supaka N., Sramala I. – Production of nisin–loaded solid lipid nanoparticles for sustained antimicrobial activity, Food Control **24** (2012) 184–190.
4. Montazer M., Shamei A., Alimohammadi F. – Stabilized nanosilver loaded nylon knitted fabric using BTCA without yellowing, Progress in Organic Coatings **74** (2012) 270–276.
5. Cheng L., Weir M. D., Xu H. H. K., Antonucci J. M., Kraigsley A. M. – Antibacterial amorphous calcium phosphate nanocomposites with a quaternary ammonium dimethacrylate and silver nanoparticles, Dental Materials **28** (2012) 561–572.
6. Lingling Zhang, Yunhong Jiang, Yulong Ding, Malcolm Povey, David York. – Investigation into the antibacterial behaviour of suspensions of ZnO nanoparticles (ZnO nanofluids), Journal of Nanoparticle Research **9** (2007) 479−489.
7. Kumar K. M., Mandal B. K., Naidu E. A. − Synthesis and Characterization of Flower Shaped Zinc Oxide Nanostructures and Its Antimicrobial Activity, Spectrochimica Acta Part A **104** (2013) 171−174.
8. Lipovsky A., Nitzan A., Gedanken Y., Lubart A. − Antifungal Activity of ZnO Nanoparticles the Role of ROS Mediated Cell Injury, Nanotechnology **22** (2011) 101−105.
9. Zhong L., Yun K. − Graphene oxide–modified ZnO particles: synthesis, characterization, and antibacterial properties, International Journal Nanomedicine **10** (2015) 79–92.
10. Padmavathy N., Vijayaraghavan R. – Enhanced bioactivity of ZnO nanoparticles–an antimicrobial study, Science and Technology of Advanced Materials **9** (3) (2008) 035–004.
11. Gu Z. J., Paranthaman P., Xu J., Pan Z. W. – Aligned ZnO nanorod arrays grown directly on zinc foils and zinc spheres by a low–temperature oxidization method, ACS Nano **3** (2) (2009) 273–278.
12. Luo Q. P., Yu X. Y., Lei B. X., Chen H. Y., Kuang D. B. – Reduced graphene oxide–hierarchical ZnO hollow sphere composites with enhanced photocurrent and photocatalytic activity, Journal of Physical Chemistry C **116** (14) (2012) 8111–8117.
13. Moleski R., Leontidis E., Krumeich F. – Controlled production of ZnO nanoparticles from zinc glycerolate in a sol–gel silica matrix, Journal of Colloid and Interface Science **302** (1) (2006) 246–253.
14. Goswami N., Sharma D. K. – Structural and optical properties of unannealed and annealed ZnO nanoparticles prepared by a chemical precipitation technique, Physica E: Low–dimensional Systems and Nanostructures **42** (5) (2010) 1675–1682.

15. Razali R., Zak A. K., Majid W. H. A., Darroudi M. – Solvothermal synthesis of microsphere ZnO nanostructures in DEA media, Ceramics International **37** (8) (2011) 3657–3663.
16. Rather J. A., Pilehvar S., Wael K. D. – A graphene oxide amplification platform tagged with tyrosinase zinc oxide quantum dot hybrids for the electrochemical sensing of hydroxylated polychlorobiphenyls, Sensors and Actuators B Chemical **190** (2014) 612–620.
17. Krishnamoorthy K., Veerapandian M., Zhang L. H., Yun K., Kim S. J. – Antibacterial efficiency of graphene nanosheets against pathogenic bacteria via lipid peroxidation, Journal of Physical Chemistry **116** (32) (2012) 17280–17287.
18. Veerapandian M., Seo Y., Yun K. S., Lee M. H., – Graphene oxide functionalized with silver@silica–polyethylene glycol hybrid nanoparticles for direct electrochemical detection of quercetin, Biosens Bioelectron **58** (2014) 200–204.
19. Kapitanova O. O., Panin G. N., Baranov A. N., Kang T. W. – Synthesis and properties of graphene oxide/graphene nanostructures, Journal of the Korean Physical Society **60** (10) (2012) 1780–1793.
20. Shen J., Yan B., Shi M., Ma H., Li N., Ye M. – Synthesis of graphene oxide–based biocomposites through diimide–activated amidation, Journal of Colloid Interface Science **356** (2) (2011) 543–549.
21. Shaobin Liu, Tingying Helen Zeng, Mario Hofmann, Ehdi Burcombe, Jun Wei, Rongrong Jiang, Jing Kong, Yuan Chen. – Antibacterial Activity of Graphite, Graphite Oxide, Graphene Oxide, and Reduced Graphene Oxide: Membrane and Oxidative Stress, ACS Nano **5** (9) (2011) 6971–6980.
22. Shahriary L. Athawale A. A. – Graphene Oxide Synthesized by using Modified Hummers Approach, International Journal of Renewable Energy and Environmental Engineering **02** (01) (2014) 58–63.
23. Flavio P., Nerina A., Tiziana M., Angela C. – Temperature influence on the synthesis of pristine graphene oxide and graphite oxide, Materials Chemistry and Physics **164** (2015) 71–77.
24. Nakajima T., Mabuchi A., Hagiwara R. – A new structure model of graphite oxide, Carbon **26** (1988) 357–361.
25. Cai D. Y., Song M. – Preparation of fully exfoliated graphite oxide nanoplatelets in organic solvents, Journal of Materials Chemistry **17** (2007) 3678–3680.
26. Tuinstra F., Koenig J. L. – Raman spectrum of graphite, Journal of Chemical Physics **53** (1970) 1126–1130.
27. Ferrari A. C., Robertson J. – Interpretation of Raman spectra of disordered and amorphous carbon, Physical Review B **61** (2000) 14095–14107.
28. Brunauer S., Emmett P. H, Teller. E. – Adsorption of gases in multimolecular layers, Journal of American Chemical Society **60** (1938) 309–319.
29. Ying Huang, Tongwen Wang, Xiaolei Zhao, Xinlong Wang, Lu Zhou, Yuanyuan Yang, Fenghui Liao, Yaqing Ju – Poly(lactic acid)/graphene oxide–ZnO nanocomposite films with good mechanical, dynamic mechanical, anti–UV and antibacterial properties, Journal of Chemical Technology and Biotechnology **90** (2014) 1677–1684.